Geosfera Indonesia
p-ISSN 2598-9723, e-ISSN 2614-8528
available online at : https://jurnal.unej.ac.id/index.php/GEOSI
Vol. 8 No. 3, December 2023, 245-261

https://doi.org/10.19184/geosi.v8i3.43360

Research Article

Application of Simple Refraction Correction Method for Shallow Coastal Bathymetric Mapping Based on UAV-Photogrammetry

I GD Yudha Partama[1] *, I Gede Gegiranang Wiryadi[1], I Dewa Gede Agung Pandawana[1], Agus Sukma Yogiswara[2]

[1] Universitas Mahasaraswati Denpasar, Jl. Kamboja No. 11A Denpasar, Bali, 80223, Indonesia
[2] Universitas Udayana, Jl. Raya Kampus Unud, Badung, Bali, 80361, Indonesia
*Corresponding author, Email address : yudhapartama@unmas.ac.id

ARTICLE INFO

Received :
18 September 2023

Revised :
1 November 2023

Accepted :
17 November 2023

Published :
21 December 2023

ABSTRACT

Shallow coastal bathymetric data has an important role in various applications, especially in maritime and coastal management fields. Various survey techniques to produce such data have been carried out by several researchers, one technique that is cheap, covers the wide area, flexible, and produces high-resolution bathymetric data is UAV-photogrammetry. However, this technique is affected by refraction effects that cause the estimated depth of underwater objects to be shallower than fact, thus reducing the accuracy of the bathymetric model. Therefore, the objective of this study is to present a simple refraction correction method based on the Ordinary Least-Square method. To test the reliability of the method, the accuracy of the model is compared with two other methods (without correction and using a correction factor = 1.34). In addition, the effectiveness of the method was also tested through its application in various survey conditions. Overall, the proposed method outperforms the two existing methods. It is also very effective in reducing the error value during high tide conditions by up to 70%. The height of the UAV does not significantly affect the accuracy of the correction model, so in this case it is recommended to use an altitude of 100 m for survey efficiency. This study demonstrated that implementing the Ordinary Least Squares method for correcting water surface refraction can enhance the precision and accuracy of UAV-photogrammetry in shallow-coastal area. In contrast to the geometric refraction correction method, the proposed technique is easier to apply and more practical.

Keywords : bathymetry; refraction effect; shallow coastal; UAV-Photogrammetry

INTRODUCTION

Shallow coastal bathymetric data is critical for a wide range of management and research applications in coastal marine settings. The water depth information is essential for port management (Mateo-Pérez et al., 2020), shipping channel consideration (DS & Subardjo, 2017), tsunami inundation modelling (Sepúlveda et al., 2020), aquaculture zoning (Landuci et al., 2020), and sediment transport analysis (Kanari et al., 2020). This data is an important component of biological oceanography in the coral reef system. The depth and characteristics of the shallow-

water bed determine the benthic organisms' habitat. These factors are essential parameters for coral reef ecosystems (Burns et al., 2015; Casella et al., 2017).

Traditionally, on-site surveying procedures such as ground-based measuring with tape measures, Total Station, and Global Positioning Systems (GPS) devices were used for collecting this data. However, because these procedures are time-consuming and labor-intensive, their spatial coverage is frequently limited (Bangen et al., 2014). Furthermore, these procedures only provide depth measurements at specific sites rather than providing continuous coverage, and they cannot simply provide bathymetric data with high spatiotemporal resolution. Advanced technologies like Light Detection and Ranging (LiDAR) offer potential for measuring depth in deeper and turbid water conditions (Kinzel et al., 2013; Marcus, 2012), but are limited by sensor availability and low spatial resolution. Ship-based multibeam ecoshounding (MBES) is costly and constrained by ship access in shallow waters (Costa et al., 2009), while boat-based mobile mapping system (BoMMS) technology has a narrow spatial footprint and is expensive for large areas (Alho et al., 2011). As a result, there is no perfect method for complete bathymetry mapping in shallow coastal areas.

As a complementary approach to conducting bathymetry in these areas, aerial photogrammetry based on stereoscopic imagery, which is a a traditional surveying technique, cost-effective and flexible method has been used to provide high spatial and temporal resolution bathymetric data in a specific area (Agrafiotis et al., 2020; Cao et al., 2020; Del Savio et al., 2023; Lingua et al., 2023; Specht et al., 2023). The recent development of computer vision-based photogrammetry techniques using structure from motion and multi view stereo (SfM-MVS) algorithms has enabled semi-automatic bathymetric measurements from aerial photos captured by digital cameras installed on unmanned aerial vehicles (UAVs) such as drones, thus facilitating data acquisition and processing, thereby reducing survey costs (Dietrich, 2017; Kholil et al., 2021; Partama et al., 2017; Woodget et al., 2015).

However, the application of this method is affected by the refraction effect on the water surface. The depth measurement seems to be shallower than the real depth due to this effect (water depth is underestimated), thus reducing the accuracy of the UAV-photogrammetry technique in mapping shallow coastal bathymetry (Dietrich, 2017; Westaway et al., 2001). Several studies have been conducted to minimise this effect, one of which is the method proposed by Westaway et al. (2001) and Woodget et al. (2015), in this method the correction factor (CF) of 1.34 (refractive index of water) is used to convert the apparent bathymetric model to the real bathymetric model. However, this CF can be applied when the effect of refraction is minimum. (i.e., camera position is close to the nadir of the target, and shallow water depth). Geometrically, this correction factor is not always ideal, the CF changes depend on the position of the stereo cameras in relation to the target point of underwater (Murase et al., 2008). However, in underwater photogrammetric measurements, it is not possible to calculate CF geometrically. Therefore, this research is aimed to proposed a simple method to correct the refraction effect based on linear regression to estimate the gain (CF) at each specific UAV flight by minimising the total error (RMSE) at the corrected depth value. In this study, the effectiveness of the method is also tested through its application in several survey conditions such as UAV altitude (50 m and 100 m) and water conditions during high and low tide.

METHODS

Study Site

The study's test site was located at Serangan Beach, Serangan Island, Denpasar-Bali (115°14'40.34"E and 8°44'10.56"S). The study area covered an estimated 272.75 m^2 based on orthophoto coverage. The beach was found to have a shallow depth ranging from 0-2 meters and a sloping terrain. The water substrate was predominantly composed of sand, coral, rocks, and seagrass. Although water transparency was not quantitatively measured, it was observed that the texture of the water bottom could be identified from aerial photographs even at the deepest

validation point, indicating good water clarity in the study area. Figure 1 provides a visual depiction of the study area overlayed on an orthophoto. The survey specifications for the study site during high and low tide conditions are detailed in Table 1.

Table 1. Specifications of each survey

Specifications	High tide	Low tide
Date of data acquisition	July19, 2023	July19, 2023
Time of day	09.15 AM	03.50 PM
Spatial coverage (m^2)	272.75	272.75
Depth range (m)	0-4.6	0-2
Water surface elevation (m)	1.5	0.15
Bottom substrat characteristics	Sand, rock, coral, and seagrass	Sand, rock, coral, and seagrass
Wave height (m)	< 0.1	< 0.1
Weather condition	sunny	sunny

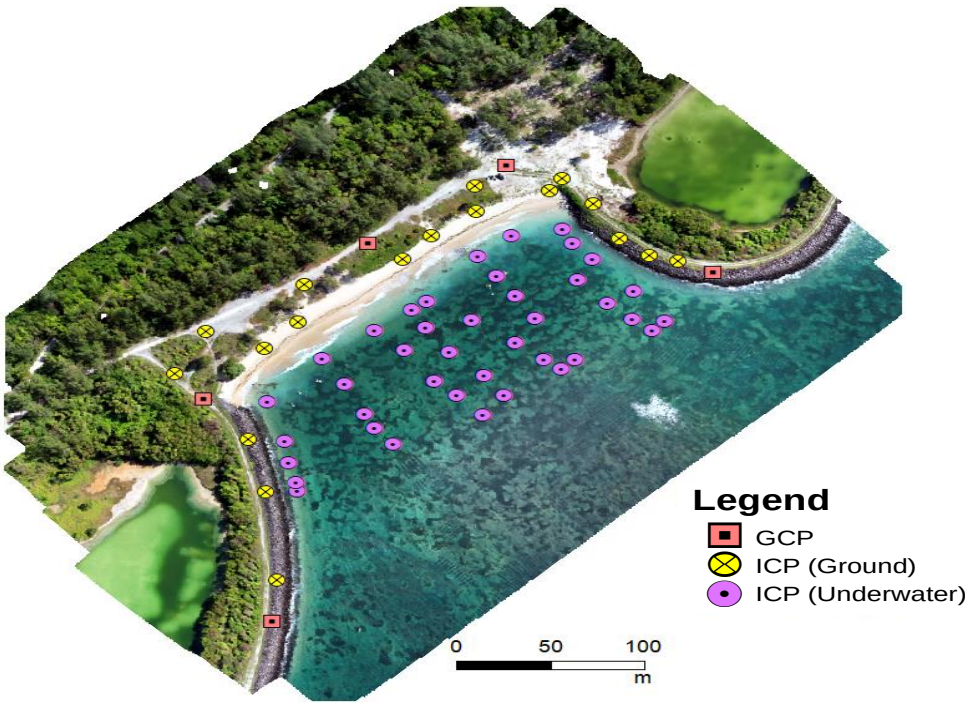

Figure 1. The study area overlayed on an orthophoto and spatial distribution of the Ground Control Point (GCP) dan Idependent Control Point (ICP)

Aerial Photos Acquisition

Aerial images were taken at high and low tides using a standard camera (4K; FOV: 88°; resolution: 5472×3648 pixels/20 MP) attached on a tiny, lightweight (595 g), quad-copter UAV (a DJI Air 2S) (Figure 2a). The drone altitude was set at 50 m and 100 m above the water surface to produce a spatial resolution of 1.5 - 3 cm, with 377 and 105 frames, respectively. The camera was programmed to automatically capture photos at each waypoint along a predetermined flight path created using Dronelink software (Figure 2b). The flight path was designed to cover areas of ground, water, as well as ICP and GCP in the aerial frames. To minimize the sunglint effect on the water surface, the camera was positioned in the nadir position. The overlapping rate for image matching in the SfM (Structure from Motion) process was set at 80% for forwardlap and 70% for

sidelap. These parameters were chosen to ensure accurate and efficient image processing (Carbonneau & Dietrich, 2017; James & Robson, 2014).

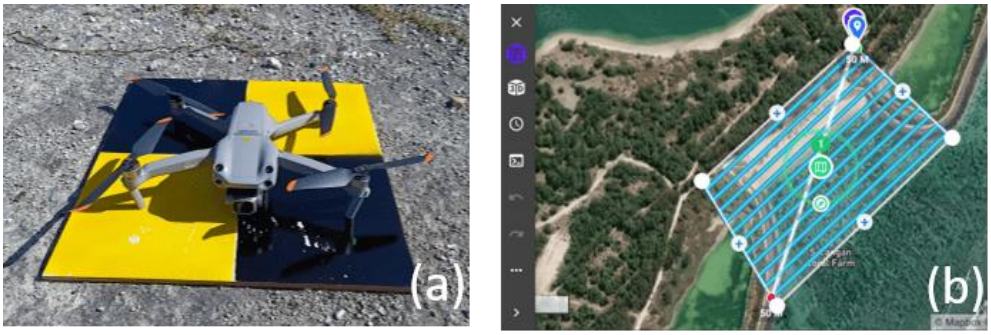

Figure 2. a) Drone DJI Air 2S and yellow-black target squares, and b) flight path created using Dronelink Software

GCP and ICP meaasurements using RTK-GNSS

Figure 1 shows the distribution of GCPs and ICPs in the study site. The GCPs were yellow-black target squares with dimensions of 40 x 40 cm and were placed on ground (Figure 2a). On the other hand, the ICPs consisted of yellow-black target for ground areas and various underwater objects such as sand, coral, rocks, and seagrass beds for submerged areas. These points' coordinates have been measured by RTK-GNSS CHCnav i50. The GCP and ground ICP coordinates were measured at the centre of the target (Figure 3a), while the submerged ICP coordinates were measured on the surface of each object (Figure 3b). The GCP coordinates were used for georeferencing and optimizing camera parameters in the photogrammetry procedure. Both ground topography and submerged topography models were validated using the ICPs. Additionally, water surface height was measured during the flight and used for depth calculation and generating a bathymetry map (Figure 3c). The study used 5 GCPs, 18 ground ICPs, and 40 submerged ICPs.

Figure 3. Coordinate measurements of GCPs and ICPs on ground (a), submerged ICPs (b), and water surface elevation (c)

Generation of Digital Surface Model of shallow-water by SfM-MVS

In this study, Agisoft Metashape Professional software was used for general SfM-MVS image processing. In the first stage, overlapping aerial photo is used as input in the image alignment and features matching process. In this stage, the SfM algorithm is used to determine the camera intrinsic and extrinsic parameters, relative camera position and sparse 3D point clouds. Furthermore, GCPs are used for the georeferencing process and optimisation of the 3D point cloud position. MVS is used to reconstruct the shape of the actual geometry resulting in a dense point

cloud (DPC) and orthophoto. To generate a topographic model/ Digital Surface Model (DSM), an interpolation process was performed on each DPC. Water areas were manually extracted for further analysis. The overall process and steps are shown in Figure 4.

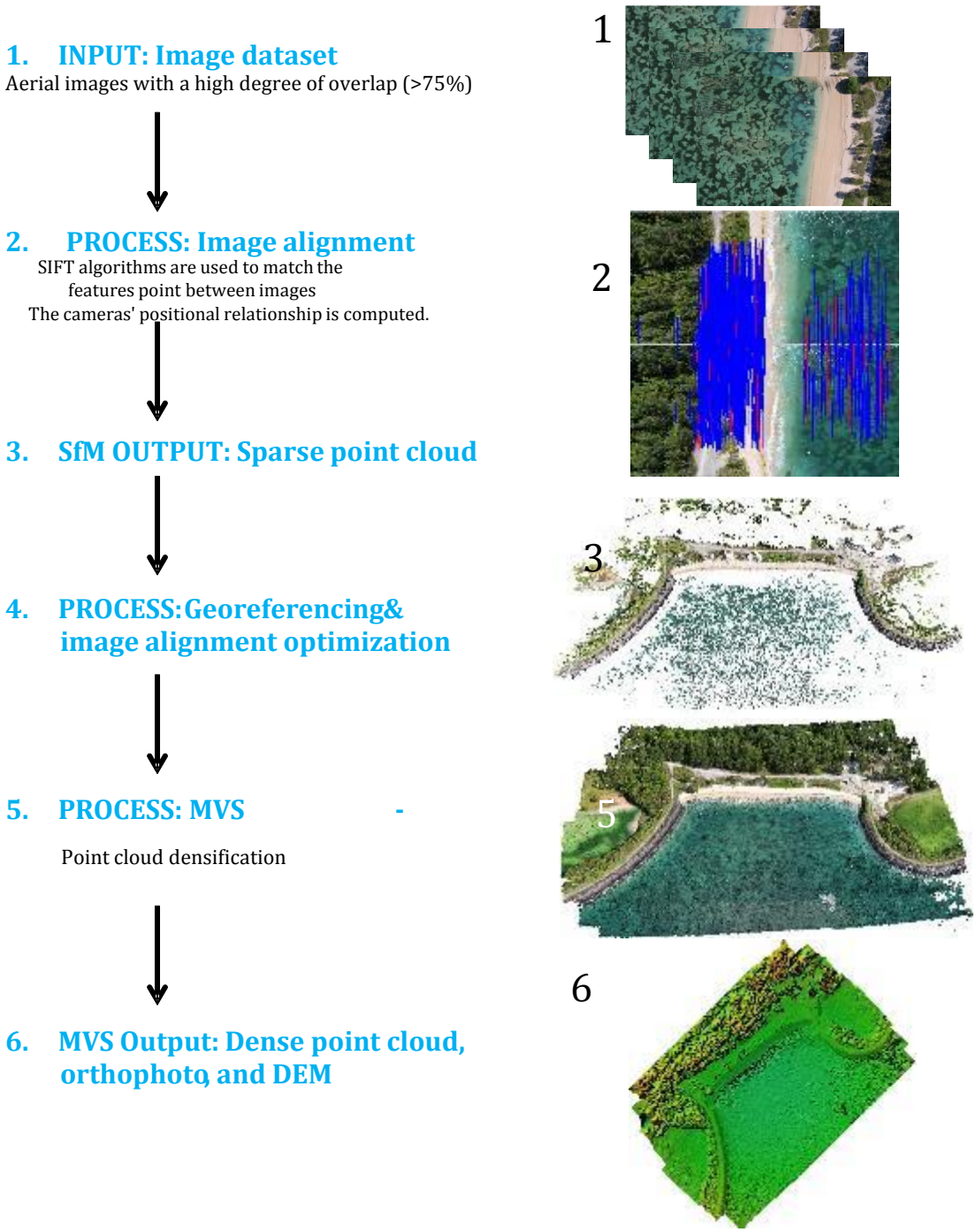

Figure 4. Overview Generation of Digital Surface Model of shallow-water by SfM-MVS

Application of Simple Empirical Refraction Correction Method

The refraction correction effect in this method is based on the equation below (1):

$$k_N = c.k_S \qquad (1)$$

Where c is the gain/correction factor (CF) of the model, k_N and k_S are the real and apparent depth calculated using the following equation:

$$\widehat{k_N} = \widehat{z_{sfc}} - z_{N,btm} \quad (2)$$

$$\widehat{k_S} = \widehat{z_{sfc}} - \widehat{z_{A,btm}} \quad (3)$$

Where $\widehat{z_{sfc}}$ is the water surface elevation, $z_{N,btm}$ is the underwater elevation measured using leveling equipment, and $\widehat{z_{A,btm}}$ is the underwater elevation estimated by photogrammetry. If we define the error of $\widehat{k_N}$ and $\widehat{k_S}$ as $\widehat{\varepsilon_N}$ and $\widehat{\varepsilon_S}$, then equation (1) can be expressed as follows:

$$\widehat{k_N} = c.\widehat{k_S} + ß \quad (4)$$

Where ß = c. $\widehat{\varepsilon_S}$ - $\widehat{\varepsilon_N}$, equation (4) is the empirical correction model of water surface refraction effect. In this study, three methods with variations of p and ß were compared under different survey conditions (drone height and tidal conditions) to produce the best model. Method 1, uses a value of p=1 and ß=0 (no refraction effect correction); Method 2 uses a value of c=1.34, while ß=0 (Westaway et al., 2001; Woodget et al., 2015) and Method 3 uses a value of c estimated using the least square method between $\widehat{k_N}$ and $\widehat{k_S}$, while ß=0 (Partama et al., 2017).

Generation of Refraction-Corrected Bathymetric map

An approach using an existing method by Woodget et al. (2015) was used to generate the refraction-corrected underwater bathymetric map. The first step in this procedure is to generate estimated apparent water depth map by subtracting the underwater apparent shallow water elevation map from the measured water surface elevation. To obtain the refraction-corrected bathymetric map, the apparent water depth map is then multiplied by the empirical refraction correction factor.

Accuracy Assessment

In general, the accuracy of the method is calculated by comparing the coordinates (XYZ) estimated using the proposed technique with the coordinates of the validation point (ICP) derived from RTK-GNSS measurements. The difference value between the model measurement and the validation point is calculated as the model estimation error. Model accuracy is assessed by comparing the total error (RMSE and ME) values of each technique/method. To validate and assess the accuracy of the underwater points using UAV-photogrammetry, first the measured water depth of the underwater ICPs using RTK-GNSS, Figure 1) is compared with the estimated water depth point on the model bathymetric map containing the point. The difference between these water depths is defined as the shallow bathymetry estimation error. Second, the cross-validation approach is used to evaluate the RMSE and ME values, which comprises of 1000 calibration/prediction trials in which the validation data is randomly divided into training and validation data. The overall accuracy standard for shallow water hydrographic mapping established by the International Hydrographic Organisation (IHO), for the vertical accuracy is ± 25 cm (Grenzdörffer & Naumann, 2016).

RESULTS AND DISCUSSION

Validity of SfM-MVS in Ground Area

Table 2 shows the the total error (RMSE) of the XYZ coordinates of the ground ICP estimated by SfM-MVS compared to the RTK-GNSS measurement for each survey condition. For the ground area, the total error for each axis is less than 0.03 m for survey condition. This value is lower than the general error in leveling equipment measurements, such as RTK-GNSS. This demonstrates the success of our photogrammetric procedure (Eker & Hübl, 2018; Harwin & Lucieer, 2012; Padro et al., 2019). Based on the table, the average error on the horizontal axis (X and Y) is smaller than the vertical axis (Z). This discrepancy can be attributed to the use of different data and spatial resolutions. The horizontal axis relies on an orthophoto with a spatial resolution of 0.015 m, while the vertical axis uses a coarser spatial resolution (0.058 m) in the form of a DSM

interpolated from the DPC model. Errors in the interpolation process contribute to the overall errors in the model (Achilleos, 2015).

Table 2. RMSE of the XYZ coordinates of the ground ICP estimated by SfM-MVS

Survey condition	Number of data	RMSE (m)				
		X	Y	Z	XYZ	XY
50 m high tide	18	0.0131	0.0087	0.0666	0.0295	0.0109
100 m high tide	18	0.0112	0.0089	0.0450	0.02196	0.0104
50 m low tide	18	0.0094	0.0088	0.0339	0.0173	0.0091
100 m low tide	18	0.0117	0.0093	0.0313	0.0174	0.0104

The Necessity of Refraction Correction in Submerged Areas

Figure 5 shows the scatter plot between estimated elevation values from SfM-MVS and RTK-GNSS measurements at various survey conditions, based on the figure most of the submerged ICP elevations estimated using SfM-MVS look shallower than RTK-GNSS measurements in both low tide and high tide conditions. The error trend is also positive as the depth increases. This is also demonstrated by the fact that the RMSE at high tide with greater depth is almost 5 times higher than at low tide. This is in line with research by Dietrich (2017), Lane et al. (2010), Shintani & Fonstad (2017), Woodget et al. (2015) which stated that the refraction effect causes an underestimation of the depth of underwater objects, thus reducing the accuracy of the SfM-MVS model and bathymetric maps.

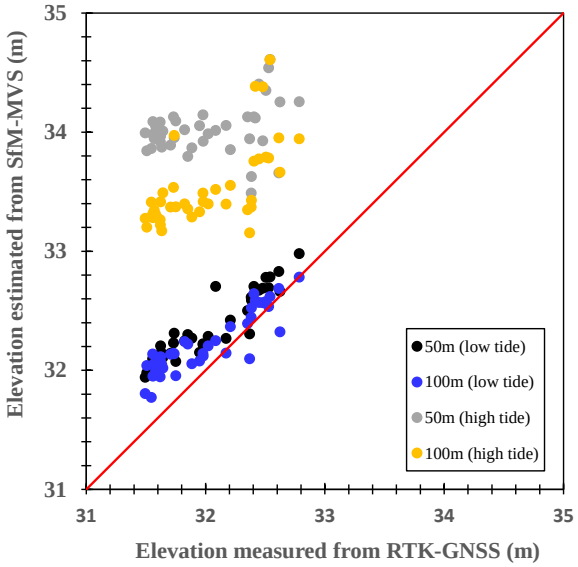

Figure 5. Scatter plot between elevation based on SfM-MVS estimation and RTK-GNSS measurement under different survey conditions

Figure 6 shows the C2C (cloud to cloud point distance) comparison of dense point clouds generated by SfM-MVS between the ground and the submerged area during high and low tide. Figure 6(a) shows that the distance between the point clouds in ground areas for the high and low tide conditions is more uniform and consistent, while the point cloud distance in the submerged area is widely spaced (indicating a change in position). In Figure 6 (b), the C2C histogram of ground area shows that the distances are mostly in the 0-0.5 m range, with an average distance of 0.436

m. In Figure 6 (c), the C2C histogram of submerged area shows that the distances are mostly in the 1.75-2 m range, with an average distance of 1.819 m. Based on these observations, it can be concluded that in submerged areas, the refraction effect on the water surface significantly affects the accuracy of object depth estimation and the reliability of the 3D model using SfM-MVS. Therefore, a correction procedure for these effects is necessary.

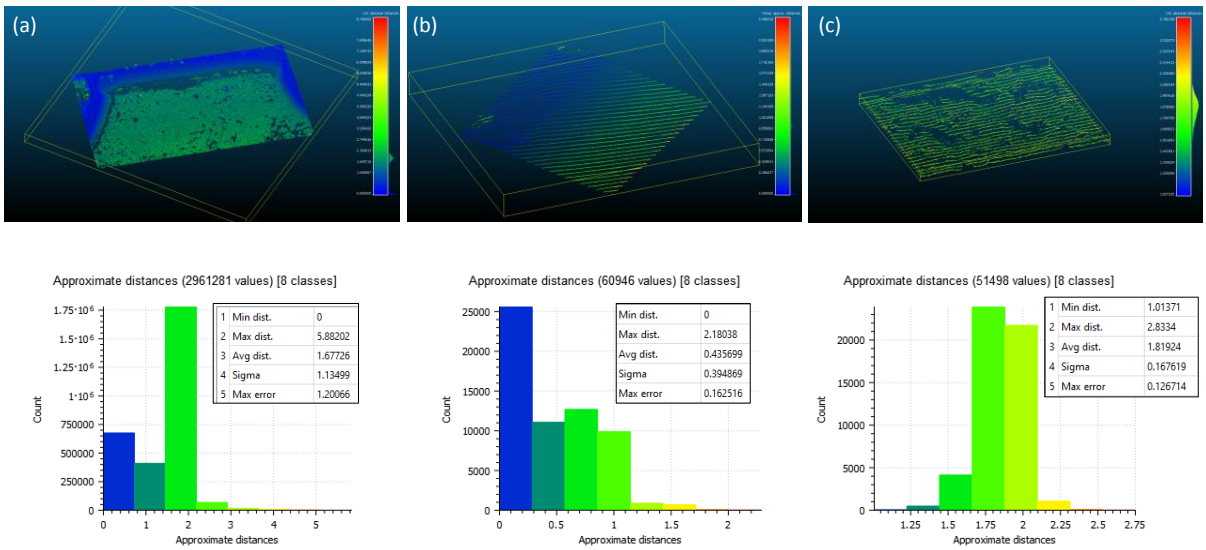

Figure 6. C2C comparison and histogram of point clouds generated from SfM-MVS a) in the whole study area; b) in the ground, and c) in the submerged area during high and low tide.

Accuracy of the Model

In Figure 5, certain elevation points at high tide have unrealistic values at both 50 and 100 m UAV altitude. This is because some of the submerged ICPs used for validation are located on the shoreline, where the photogrammetric process is disrupted by the white-water effect of the waves. As a result, this effect causes significant problems during the feature matching process and contributes to outliers in the generation of DPCs. The impact of this effect is also observed in the bathymetry map created during high tide conditions, where the elevation values in the nearshore area are highly unrealistic (Figure 9). Due to these factors, certain points/ICPs located in this area were not included in the accuracy test of the refraction correction model.

Figures 7 shows the error assessment (RMSE/ME) by cross validation for each method and survey conditions. During high tide conditions, the higher spatial resolution model (50 m drone height) had lower accuracy than the lower spatial resolution model (100 m drone height) (Figure 3a). This was attributed to the wave effect, where the wave pattern had significant systematic effects on the location of water bottom objects. Even in calm sea conditions, the lateral displacement caused by the waves could reach up to 30 cm at 5 m water depth (Agrafiotis et al., 2019). This displacement increased as the camera height decreased, leading to mis-estimation of the bottom object and reduced model accuracy (Fryer & Kniest, 2006). However, at low tide with a water depth of less than 1.4 m, the wave effect was not significant (Figure 7b).

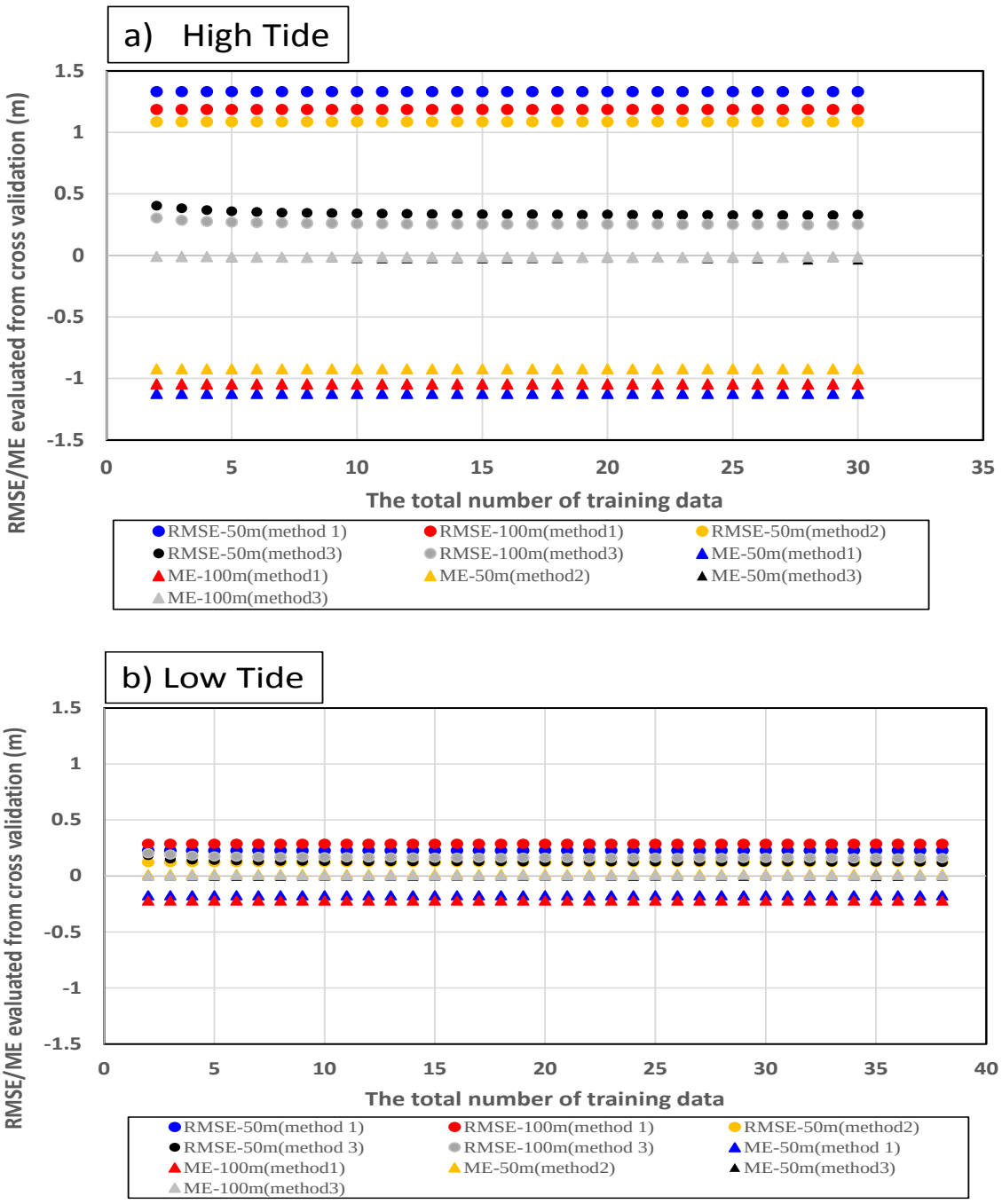

Figure 7. Error assessment (RMSE/ME) by cross validation for each method and survey conditions; (a) high tide and (b) low tide

Based on Figure 7a, overall, Method 1 produces the largest values of RMSE and ME due to systematic underestimation (reflected in large negative ME) caused by neglecting the refraction effect. This result demonstrates the necessity for implementing a refraction correction procedure in the bathymetric model. As a result of a simple correction for the refraction effect using CF = 1.34 (Westaway et al., 2001), method 2 produces RMSE approximately 22% lower than method 1, but there is still suffered from a significant systematic underestimation (i.e., negative, and large ME values). This demonstrates the geometric fact that a correction factor of 1.34 is the minimum possible value and is not enough for practical applications.

In terms of bathymetric model accuracy, Method 3 outperformed Methods 1 and 2 (RMSE and ME values are much lower than methods 1 and 2 at high tide), showing the effectiveness of

the method in reducing the refraction effect. Additionally, compared to the approaches suggested by Butler et al. (2002) and Murase et al. (2008), this method shows higher overall accuracy. Furthermore, this empirical linear regression method corrects for other effects in addition to the refraction effect. For example, it corrects for systematic errors in DEM resulting from inaccurate estimation of the camera parameters (intrinsic and extrinsic) by the SfM algorithm, as well as position and orientation (Hsu & Wang, 2011).

The experiment suggested by Kanno et al. (2018) provides one example of how the refraction effect of water surface can be mitigated using an empirical linear regression approach. Using computer-based visual modeling, they offered the ideal correction factor for a range of geometries in this experiment. Every combination of overlap rate and altitude was tested through simulation. The experiment shows that at high enough overlap rates, there is a minimal variability of the correction factor as displayed by the narrow quartile widths. This indicates that the refraction effect of the entire model can be corrected using a single correction factor value, regardless of the bottom texture and altitude.

Furthermore, in this method, the total eror (RMSE and ME) increase as the number of training data decreases, but it is not very significant when the number of training data is greater than 5. Therefore, it can be suggested that the minimum number of training data in generating a correction model to predict CF values is at least 5.

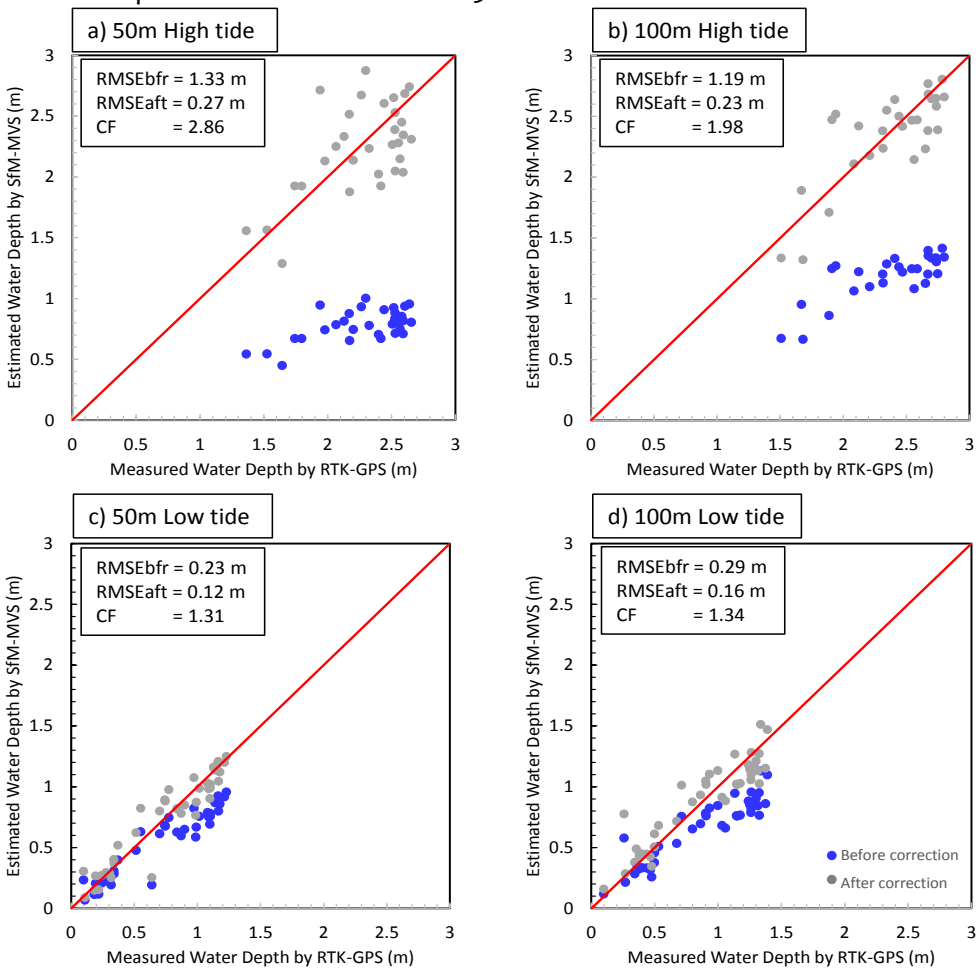

Figure 8. Scatter plot between depth based on SfM-MVS estimation and RTK-GNSS measurement under various survey conditions, before and after the application of refraction correction: a) 50m-high tide; b) 100m-high tide; c) 50m-low tide; d) 100m-low tide.

In this study, Method 3 was tested under several survey conditions to determine the reliability of the method. Firstly, the method was tested at different UAV altitudes during aerial data collection. In high tide conditions, a height of 100 m is recommended due to the squeezing effect described above. However, during low tide conditions, the RMSE and ME values at the two heights did not have a significant effect (Figure 7b). In addition, as shown in Table 3, at high tide condition, a height of 50 m has larger error (about 67.8% of the depth at deepest area) than a height of 100 m (about 52% of the depth at deepest area). On the other hand, at low tide condition, a height of 50 m has no significant different of error (about 28.6% of the depth in average) with the height of 100 m (about 27.6% of the depth in average). In this study, it is recommended to use an altitude of 100 m. This is because at this altitude, the amount of aerial data collected is less, so the process of collecting and processing photogrammetric data will be more effective.

Table 3. Depth errors for through-water photogrammetry at different conditions (tide and UAV height), Maximum, and RMSE shown as a percentage of depth

Tide condition	**Low tide**					
Flying height		50 m			100 m	
Water depth (m)	Max (m)	RMSE (m)	RMSE (%)	Max (m)	RMSE (m)	RMSE (%)
0 - 0.5	-0.1226	0.0739	29.7037	-0.2169	0.1334	35.7779
0.5 – 1	-0.4441	0.2298	29.2388	-0.1648	0.1245	15.3238
1 - 1.5	-0.4070	0.3048	26.9093	-0.5610	0.3953	31.8049
Tide condition	**High tide**					
Flying height		50 m			100 m	
Water depth (m)	Max (m)	RMSE (m)	RMSE (%)	Max (m)	RMSE (m)	RMSE (%)
1.5 – 2	-1.2340	1.1032	62.3183	-1.0231	0.8639	48.2715
2 - 2.5	-1.7443	1.4625	64.6917	-1.2479	1.0971	47.7540
2.5 – 3	-1.8790	1.7411	67.8075	-1.5414	1.3975	52.0664

In addition, Figure 9 demonstrates the relationship between estimated bottom elevation error and water depth for the uncorrected and corrected models at high tide. For uncorrected models, estimated bottom elevation error typically increased linearly with increasing water depth. This is also confirmed by the high slope and R^2 of the regression line. In addition to the water's refractive index, other variables, such bed texture, also played a role in determining the linear relationship between estimated bottom elevation error and water depth (Zhang et al., 2022). For the corrected model, the error does not appear to increase with increasing water depth, and the slope and R^2 of the regression line are insignificant. Therefore, a simple empirical correction model can be used at different UAV heights and tide conditions. Overall, there are no issues with implementing the simple empirical correction model for underwater areas with varying depths (Partama et al., 2020).

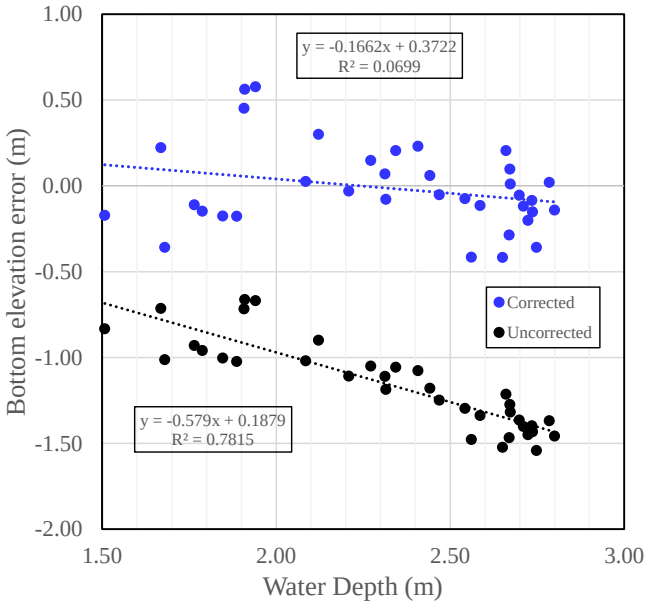

Figure 9. Relationship between estimated bottom elevation error and water depth for uncorrected and corrected models at high tide by photogrammetry

Secondly, the method was tested at different tide conditions. The model was found to reduce error values by 70% under high tide (Figure 7a) and 20% under low tide (Figure 7b). However, the average RMSE value at low tide is much lower (0.166 m) than at high tide (0.254 m). In accordance with hydrographic survey regulations, for special orders with shallow water conditions, the recommended depth accuracy level is less than 0.25 m (Grenzdörffer & Naumann, 2000; Nugroho et al., 2022), therefore the error value in the study is still tolerable. This suggests that the simple empirical correction method used in the study can be applied in various water conditions, both high and low tide. A scatter plot comparing the depth estimation based on the model with actual measurements before and after applying the correction method showed that the correction significantly improved the accuracy of the bathymetry model (Figure 8). Overall, the study concludes that the simple refraction effect correction method, based on the Least Square method, is highly effective in improving the accuracy of the water depth estimation.

Corrected Bathymetry Map

The bathymetry map was created by extracting the submerged area from the DSM generated by SfM-MVS. The submerged DSM was then adjusted for refraction effects using method 3. Figure 10 shows the bathymetry map at high and low tide with variations in drone height. In Figures 10a and 10b the accuracy of the estimated depth at shoreline is compromised due to the squeezing effect at high tide. The histogram also shows unrealistic depth distribution values during high tide ranging from -8 to 4 m compared to the low tide condition ranging from 0 to 2 m. The quality of the bathymetric map is degraded for two reasons. First, at the shoreline, the wave breaking causes the white-water and foam zone directly, thus making obscures features on the seafloor. Second, the location of the foam patterns in the white water moves, causing areas on the seafloor to be visible in some images, but not in others. These two issues cause SfM to fail to efficiently match and align images properly and therefore, map seafloor depths (Agrafiotis et al., 2020; Grenzdörffer & Naumann, 2016). In order to obtain accurate bathymetric maps, it is important to consider the optimum survey conditions, such as imagery acquisitions should be conducted during the calmest conditions possible. This planning includes flying when waves are the smallest seasonally, and adjusting flying locations based on real time weather and wave conditions (Slocum et al., 2019).

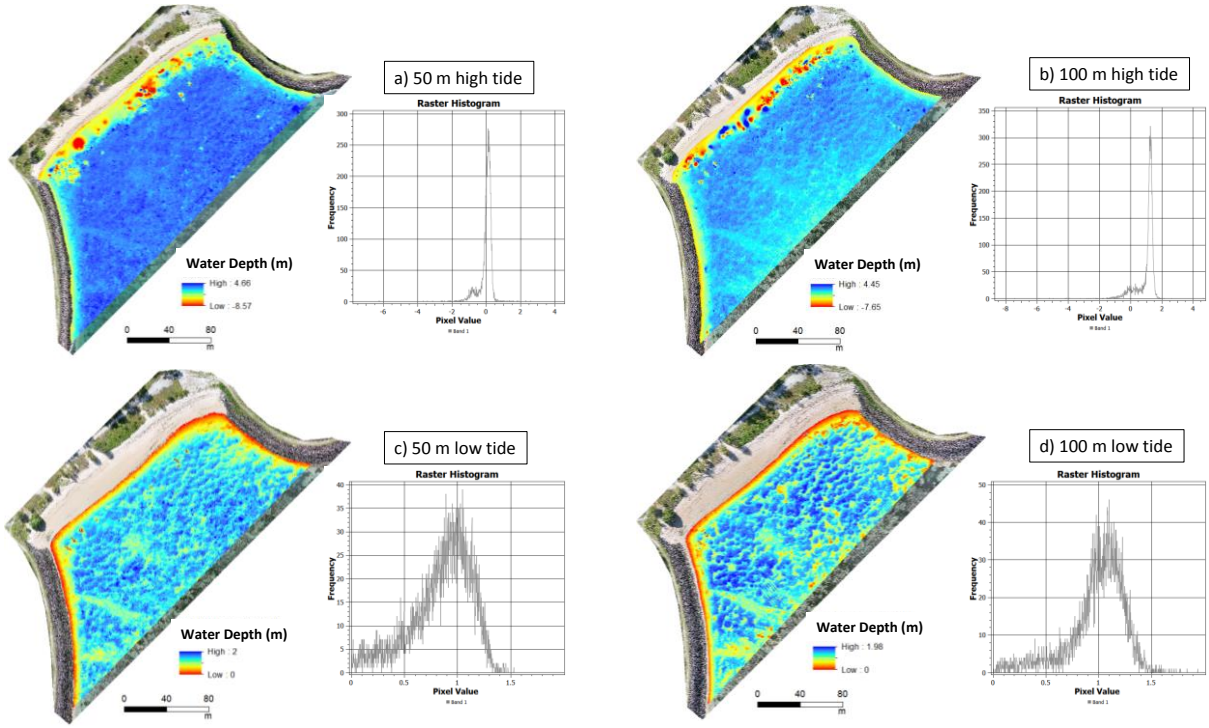

Figure 10. Shallow-coastal bathymetric maps at various survey conditions: a) 50m-high tide; b) 100m-high tide; c) 50m-low tide after correction, and d) 100m-low tide after correction.

CONCLUSION

Generally, the presented simple refraction correction that implementing the Ordinary Least Squares method can improve the precision and accuracy of UAV-photogrammetry in shallow-coastal area. The presented method outperforms two existing methods: the uncorrected approach (method 1) and the method using the refractive index of water (1.34) as CF (method 2). This demonstrates the geometric fact that a correction factor based on this index is the minimum possible value and is not enough for practical applications. Under tidal conditions, the method has good effectiveness, especially at high tide, where it can improve accuracy by up to 70%. The height of the drone has a significant effect on the accuracy of the model, especially during high tide conditions, where low drone height can cause lateral displacement effects that reduce accuracy, while during low tide conditions, drone height does not have a significant effect on accuracy. For this reason, this research recommends using an altitude of 100 m as an efficient way to acquire and process aerial data using photogrammetry. In order to obtain accurate bathymetric maps, it is important to consider the optimum survey conditions, such as imagery acquisitions should be conducted during the calmest conditions possible. This planning includes flying when waves are the smallest seasonally, and adjusting flying locations based on real time weather and wave conditions.

ACKNOWLEDGMENTS

This work was supported by The Ministry of Education, Culture, Research, and Technology of Indonesia (Grant Number: 184/E5/PG.02.00.PL/2023).

DECLARATIONS

Conflict of Interest

The authors declared that they had no known competing interests.

Ethical Approval
On behalf of all authors, the corresponding author states that the paper satisfies Ethical Standards conditions, no human participants, or animals are involved in the research.

Informed Consent
On behalf of all authors, the corresponding author states that no human participants are involved in the research and, therefore, informed consent is not required by them.

DATA AVAILABILITY

Data used to support the findings of this study are available from the corresponding author upon request.

REFERENCES

Achilleos, G. A. (2015). Interpolation and elevation errors: the impact of the DEM resolution. In Third International Conference on Remote Sensing and Geoinformation of the Environment (RSCy2015) (Vol. 9535, pp. 212-221). SPIE.

Agrafiotis, P., Skarlatos, D., Georgopoulos, A., & Karantzalos, K. (2019). Shallow water bathymetry mapping from UAV imagery based on machine learning. *The International Archives of the Photogrammetry, Remote Sensing and Spatial Information Sciences*, XLII-2(W10).

Agrafiotis, P., Karantzalos, K., Georgopoulos, A., & Skarlatos, D. (2020). Correcting image refraction: Towards accurate aerial image-based bathymetry mapping in shallow waters. *Remote Sensing, 12*(2), 322. https://doi.org/10.3390/rs12020322.

Alho, P., Vaaja, M., Kukko, A., Kasvi, E., Kurkela, M., Hyyppä, J., . . . Kaartinen, H. (2011). Mobile laser scanning in fluvial geomorphology: Mapping and change detection of point bars. *J Zeitschrift fur Geomorphologie-Supplementband, 55*(2), 31.

Bangen, S. G., Wheaton, J. M., Bouwes, N., Bouwes, B., & Jordan, C. (2014). A methodological intercomparison of topographic survey techniques for characterizing wadeable streams and rivers. *Geomorphology, 206*, 343-361. https://doi.org/10.1016/j.geomorph.2013.10.010.

Burns, J. H. R., Delparte, D., Gates, R. D., & Takabayashi, M. (2015). Integrating structure-from-motion photogrammetry with geospatial software as a novel technique for quantifying 3D ecological characteristics of coral reefs. *PeerJ, 3*, e1077. https://doi.org/10.7717/peerj.1077.

Butler, J., Lane, S., Chandler, J., & Porfiri, E. (2002). Through-water close range digital photogrammetry in flume and field environments. *The Photogrammetric Record, 17*(99), 419-439. https://doi.org/10.1111/0031-868X.00196.

Cao, B., Deng, R., & Zhu, S. (2020). Universal algorithm for water depth refraction correction in through-water stereo remote sensing. *International Journal of Applied Earth Observation and Geoinformation, 91*, 102108. https://doi.org/10.1016/j.jag.2020.102108.

Carbonneau, P. E., & Dietrich, J. T. (2017). Cost-effective non-metric photogrammetry from consumer-grade sUAS: implications for direct georeferencing of structure from motion photogrammetry. *Earth surface processes and landforms, 42*(3), 473-486. https://doi.org/10.1002/esp.4012.

Casella, E., Collin, A., Harris, D., Ferse, S., Bejarano, S., Parravicini, V., ... & Rovere, A. (2017). Mapping coral reefs using consumer-grade drones and structure from motion photogrammetry techniques. *Coral Reefs, 36*, 269-275. https://doi.org/10.1007/s00338-016-1522-0.

Costa, B. M., Battista, T. A., & Pittman, S. J. (2009). Comparative evaluation of airborne LiDAR and ship-based multibeam SoNAR bathymetry and intensity for mapping coral reef ecosystems. *Remote Sensing of Environment, 113*(5), 1082-1100. https://doi.org/10.1016/j.rse.2009.01.015.

Del Savio, A. A., Luna Torres, A., Vergara Olivera, M. A., Llimpe Rojas, S. R., Urday Ibarra, G. T., & Neckel, A. (2023). Using UAVs and Photogrammetry in Bathymetric Surveys in Shallow Waters. *Applied Sciences, 13*(6), 3420. https://doi.org/10.3390/app13063420.

Dietrich, J. T. (2017). Bathymetric structure-from-motion: Extracting shallow stream bathymetry from multi-view stereo photogrammetry. *Earth Surface Processes and Landforms, 42*(2), 355-364. https://doi.org/10.1002/esp.4060.

DS, A. A., & Subardjo, P. (2017). Bathymetry mapping study as a consideration in determining shipping channel in pramuka island waters, seribu islands, DKI Jakarta. *International Journal of Marine Aquatic Resource Conservation Co-existence, 2*(1), 12-17. https://doi.org/10.14710/gt.v%25vi%25i.16876.

Eker, R., Aydın, A., & Hübl, J. (2018). Unmanned aerial vehicle (UAV)-based monitoring of a landslide: Gallenzerkogel landslide (Ybbs-Lower Austria) case study. *Environmental monitoring and assessment, 190*, 1-14. https://doi.org/10.1007/s10661-017-6402-8.

Fryer, J. G., & Kniest, H. T. (1985). Errors in depth determination caused by waves in through-water photogrammetry. *The Photogrammetric Record, 11*(66), 745-753. https://doi.org/10.1111/j.1477-9730.1985.tb01326.x.

Grenzdörffer, G. J., & Naumann, M. (2016). Investigations on the Possibilities of Monitoring Coastal Changes Including Shallow Under Water Areas With Uas Photo Bathmetry. The International Archives of the Photogrammetry, Remote Sensing and Spatial Information Sciences, 41, 843-850.

Harwin, S., & Lucieer, A. (2012). Assessing the accuracy of georeferenced point clouds produced via multi-view stereopsis from unmanned aerial vehicle (UAV) imagery. *Remote Sensing, 4*(6), 1573-1599. https://doi.org/10.3390/rs4061573.

Hsu, P. H., & Wang, C. K. (2011, December). Acquiring underwater DSM using close-range photogrammetry. In 32nd Asian Conference on Remote Sensing 2011, ACRS 2011 (pp. 267-272).

James, M. R., & Robson, S. (2014). Mitigating systematic error in topographic models derived from UAV and ground-based image networks. *Earth Surface Processes and Landforms, 39*(10), 1413-1420. https://doi.org/10.1002/esp.3609.

Kanari, M., Tibor, G., Hall, J. K., Ketter, T., Lang, G., & Schattner, U. (2020). Sediment transport mechanisms revealed by quantitative analyses of seafloor morphology: New evidence from multibeam bathymetry of the Israel exclusive economic zone. *Marine and Petroleum Geology, 114*, 104224. https://doi.org/10.1016/j.marpetgeo.2020.104224.

Kanno, A., Yonehara, C., Partama, I.G.Y., Komuro, T., Inui, R., Goto, M., Akamatsu, Y. (2018). A Study on Water Surface Refraction Correction Coefficients for Photogrammetric Survey of Flooded Riverbeds Using UAV and SfM-MVS. *Journal of River Engineering, 24*, 19-24.

Kholil, M., Ismanto, I., & Fu'Ad, M. (2021). 3D reconstruction using structure from motion (SFM) algorithm and multi view stereo (MVS) based on computer vision. Paper presented at the IOP Conference Series: Materials Science and Engineering.

Kinzel, P. J., Legleiter, C. J., & Nelson, J. M. (2013). Mapping river bathymetry with a small footprint green LiDAR: applications and challenges 1. *JAWRA Journal of the American Water Resources Association, 49*(1), 183-204. https://doi.org/10.1111/jawr.12008.

Landuci, F. S., Rodrigues, D. F., Fernandes, A. M., Scott, P. C., & Poersch, L. H. D. S. (2020). Geographic Information System as an instrument to determine suitable areas and identify suitable zones to the development of emerging marine finfish farming in Brazil. *Aquaculture Research, 51*(8), 3305-3322. https://doi.org/10.1111/are.14666

Lane, S. N., Widdison, P. E., Thomas, R. E., Ashworth, P. J., Best, J. L., Lunt, I. A., ... & Simpson, C. J. (2010). Quantification of braided river channel change using archival digital image analysis. *Earth Surface Processes and Landforms, 35*(8), 971-985. https://doi.org/10.1002/esp.2015.

Lingua, A. M., Maschio, P., Spadaro, A., Vezza, P., & Negro, G. (2023). Iterative Refraction-Correction Method on Mvs-Sfm for Shallow Stream Bathymetry. The International Archives of the Photogrammetry, Remote Sensing and Spatial Information Sciences, 48, 249-255.

Marcus, W. A. (2012). Remote sensing of the hydraulic environment in gravel-bed rivers. *Gravel-bed rivers: Processes, tools, environments*, 259-285. https://doi.org/10.1002/9781119952497.ch21.

Mateo-Pérez, V., Corral-Bobadilla, M., Ortega-Fernández, F., & Vergara-González, E. P. (2020). Port bathymetry mapping using support vector machine technique and sentinel-2 satellite imagery. *Remote sensing, 12*(13), 2069. https://doi.org/10.3390/rs12132069

Murase, T., Tanaka, M., Tani, T., Miyashita, Y., Ohkawa, N., Ishiguro, S., . . . Yamano, H. (2008). A photogrammetric correction procedure for light refraction effects at a two-medium boundary. Photogrammetric engineering remote sensing, 74(9), 1129-1136. https://doi.org/10.14358/PERS.74.9.1129.

Nugroho, C., Manik, H., Gultom, D., & Firdaus, M. (2022). Implementasi multibeam echosounder untuk pengukuran dan analisis data kedalaman Perairan Teluk Jakarta berdasarkan Standar International Hydrographic Organization. POSITRON, 12(1), 60-71. http://dx.doi.org/10.26418/positron.v12i1.51833.

Padró, J. C., Muñoz, F. J., Planas, J., & Pons, X. (2019). Comparison of four UAV georeferencing methods for environmental monitoring purposes focusing on the combined use with airborne and satellite remote sensing platforms. *International journal of applied earth observation and geoinformation, 75*, 130-140. https://doi.org/10.1016/j.jag.2018.10.018.

Partama, I. G. Y., Kanno, A., Akamatsu, Y., Inui, R., Goto, M., & Sekine, M. (2017). A simple and empirical refraction correction method for UAV-based shallow-water photogrammetry. International Journal of Geological Environmental Engineering, 11(4), 295-302.

Partama, I. G. Y., Sumantra, I. K., WP, A. S., & Yogiswara, A. S. (2020). Validation of high-resolution and simple river monitoring technique using UAV-SFM Method. *International Journal of Recent Technology and Engineering, 8*(5), 5409-5414.

Sepúlveda, I., Tozer, B., Haase, J. S., Liu, P. L. F., & Grigoriu, M. (2020). Modeling uncertainties of bathymetry predicted with satellite altimetry data and application to tsunami hazard assessments. *Journal of Geophysical Research: Solid Earth, 125*(9), e2020JB019735. https://doi.org/10.1029/2020JB019735.

Shintani, C., & Fonstad, M. A. (2017). Comparing remote-sensing techniques collecting bathymetric data from a gravel-bed river. *International journal of remote sensing, 38*(8-10), 2883-2902. https://doi.org/10.1080/01431161.2017.1280636.

Slocum, R. K., Wright, W., Parrish, C., Costa, B., Sharr, M., & Battista, T. A. (2019). Guidelines for bathymetric mapping and orthoimage generation using sUAS and SfM, an approach for conducting nearshore coastal mapping. National Oceanic and Atmospheric Administration. https://doi.org/10.25923/07mx-1f93

Specht, M., Szostak, B., Lewicka, O., Stateczny, A., & Specht, C. (2023). Method for determining of shallow water depths based on data recorded by UAV/USV vehicles and processed using the SVR algorithm. *Measurement, 221*, 113437. https://doi.org/10.1016/j.measurement.2023.113437.

Westaway, R. M., Lane, S. N., Hicks, D. M. J. P. E., & Sensing, R. (2001). Remote sensing of clear-water, shallow, gravel-bed rivers using digital photogrammetry. *Photogrammetric engineering remote sensing, 67*(11), 1271-1282.

Woodget, A. S., Carbonneau, P. E., Visser, F., & Maddock, I. P. (2015). Quantifying submerged fluvial topography using hyperspatial resolution UAS imagery and structure from motion photogrammetry. *Earth surface processes and landforms, 40*(1), 47-64. https://doi.org/10.1002/esp.3613.

Zhang, C., Sun, A. R., Hassan, M. A., & Qin, C. (2022). Assessing through-water structure-from-motion photogrammetry in gravel-bed Rivers under controlled conditions. *Remote Sensing, 14*(21), 5351. https://doi.org/10.3390/rs14215351.